Altered lung phospholipid metabolism in mice with targeted deletion of lysosomal-type phospholipase A_2[1]

Aron B. Fisher,[2,*] Chandra Dodia,[*] Sheldon I. Feinstein,[*] and Ye-Shih Ho[†]

Institute for Environmental Medicine,[*] University of Pennsylvania Medical Center, Philadelphia, PA; and Institute of Environmental Health Sciences,[†] Wayne State University, Detroit, MI

Abstract **Lung surfactant dipalmitoylphosphatidylcholine (DPPC) is endocytosed by alveolar epithelial cells and degraded by lysosomal-type phospholipase A_2 (aiPLA$_2$). This enzyme is identical to peroxiredoxin 6 (Prdx6), a bifunctional protein with PLA$_2$ and GSH peroxidase activities. Lung phospholipid was studied in Prdx6 knockout (Prdx6$^{-/-}$) mice. The normalized content of total phospholipid, phosphatidylcholine (PC), and disaturated phosphatidylcholine (DSPC) in bronchoalveolar lavage fluid, lung lamellar bodies, and lung homogenate was unchanged with age in wild-type mice but increased progressively in Prdx6$^{-/-}$ animals. Degradation of internalized [^{3}H]DPPC in isolated mouse lungs after endotracheal instillation of unilamellar liposomes labeled with [^{3}H]DPPC was significantly decreased at 2 h in Prdx6$^{-/-}$ mice (13.6 ± 0.3% vs. 26.8 ± 0.8% in the wild type), reflected by decreased dpm in the lysophosphatidylcholine and the unsaturated PC fractions. Incorporation of [^{14}C]palmitate into DSPC at 24 h after intravenous injection was decreased by 73% in lamellar bodies and by 54% in alveolar lavage surfactant in Prdx6$^{-/-}$ mice, whereas incorporation of [^{3}H]choline was decreased only slightly. Phospholipid metabolism in Prdx6$^{-/-}$ lungs was similar to that in wild-type lungs treated with MJ33, an inhibitor of aiPLA$_2$ activity. These results confirm an important role for Prdx6 in lung surfactant DPPC degradation and synthesis by the reacylation pathway.**—Fisher, A. B., C. Dodia, S. I. Feinstein, and Y-S. Ho. **Altered lung phospholipid metabolism in mice with targeted deletion of lysosomal-type phospholipase A_2. *J. Lipid Res.* 2005.** 46: **1248–1256.**

Supplementary key words peroxiredoxin 6 • lung surfactant • dipalmitoylphosphatidylcholine • phospholipid remodeling • phospholipid synthesis

Lung surfactant is a phospholipid-protein complex that is secreted by lung epithelium and functions to maintain alveolar stability. The major surface-active phospholipid in lung surfactant is dipalmitoylphosphatidylcholine (DPPC), which constitutes ~50% of surfactant mass (1). DPPC is synthesized and secreted by exocytosis of lamellar bodies from granular pneumocytes (alveolar type 2 epithelial cells), whereas "spent" DPPC is removed from the alveolar space by endocytosis, predominantly by the granular pneumocytes, and is either resecreted or degraded (1, 2). Under basal conditions, the turnover of alveolar DPPC is ~5%/h (2).

Previous studies have indicated that hydrolysis by phospholipase A_2 (PLA$_2$) is the major degradative pathway for internalized alveolar DPPC (3–6). MJ33, a transition-state analog competitive inhibitor of PLA$_2$ (7), inhibited the degradation of DPPC by ~50% in both the whole lung and isolated alveolar type 2 cells (3, 6). In vitro measurement of PLA$_2$ activity in homogenate of lungs or isolated type 2 cells was markedly inhibited by MJ33 when assayed at pH 4.0 in Ca^{2+}-free medium but had no effect on Ca^{2+}-dependent PLA$_2$ activity at pH 8.5 (3, 6). Based on the acidic pH optimum, we postulated that activity inhibited by MJ33 represented a lysosomal-type PLA$_2$ (aiPLA$_2$) (6).

We subsequently used column chromatography to isolate a protein from rat and bovine lungs that showed the characteristic properties of aiPLA$_2$ (8). After partial sequence analysis by mass spectroscopy, we identified a full-length human cDNA sequence in GenBank that, when expressed in either a cellular or a cell-free system, exhibited aiPLA$_2$ activity (8). This was the first lysosomal PLA$_2$ to have been sequenced. Further study indicated that the protein had homology to the peroxiredoxin family of antioxidant enzymes, and was identical to peroxiredoxin 6 (Prdx6), a nonseleno protein with glutathione peroxidase activity (9–11). We have shown by site-directed mutagenesis that the peroxidase and PLA$_2$ enzymatic functions of this protein have distinctly different active sites; the PLA$_2$ activity is Ser32-dependent, whereas the peroxidase activity requires Cys47 (12). Both we and another group have indepen-

Manuscript received 17 December 2004 and in revised form 23 February 2005.

Published, JLR Papers in Press, March 16, 2005.
DOI 10.1194/jlr.M400499-JLR200

[1] These results were presented in preliminary form at the Experimental Biology meeting in Washington, DC, in April 2004, the FASEB Surfactant Conference in Saxtons River, VT, in July 2004, and the 2nd International Symposium on Phospholipases A_2 in Berlin, Germany, in October 2004.

[2] To whom correspondence should be addressed.
e-mail: abf@mail.med.upenn.edu

dently developed Prdx6 gene-targeted mice (13, 14). The mice are viable and reproduce normally (13, 14) but show increased sensitivity to oxidant stresses, such as exposure to paraquat (14) or hyperoxia (15). In the present study, we evaluated surfactant phospholipid metabolism in lungs from Prdx6 knockout ($Prdx6^{-/-}$) mice to investigate further the PLA_2 activity of this protein.

MATERIALS AND METHODS

Materials

Authentic lipids were purchased from Avanti Polar Lipids (Birmingham, AL). Radiochemicals were purchased from Perkin Elmer Life Science (Boston, MA). BSA and fatty acid-free BSA were obtained from Roche Diagnostics (Indianapolis, IN). Ham's F-12 medium was purchased from Invitrogen Life Technologies (Carlsbad, CA). Plastic tissue culture dishes were purchased from Costar (Cambridge, MA). Dispase, mouse serum, and other tissue culture reagents were purchased from Sigma (St. Louis, MO). Thin-layer chromatography plates (Whatman), neutral alumina, osmium tetroxide, and organic solvents were purchased from Fisher Scientific (Pittsburgh, PA). Fixatives and strains for lung morphology were purchased from Electron Microscopy Sciences (Fort Washington, PA). MJ33 was a gift from Dr. Mahendra Jain (University of Delaware, Newark, DE).

Animals and cell isolation

$Prdx6^{-/-}$ mice were generated in the animal care facilities at the University of Pennsylvania by breeding $Prdx6^{+/-}$ mice. As described previously (13), the null mice developed normally and showed no obvious physical differences from their heterozygous or $Prdx6^{+/+}$ littermates. The mice used for this study represent the first-generation offspring of $Prdx6^{-/-}$ matings. Because the knockout had been produced by microinjection of cloned 129SvJ cells into C57BL/6J blastocysts (13), wild-type mice of these strains were purchased from The Jackson Laboratory (Bar Harbor, ME) and maintained in our animal care facility for 1 week for use as a control. The analysis of phenotype (lung phospholipid pool size) showed no difference between these two strains, and subsequent metabolic studies were carried out only with the C57BL/6 mice as a control. Unless specified otherwise, mice were used at 23–25 g body weight (age, 9–11 weeks). A small number of $Prdx6^{-/-}$ and wild-type mice were maintained in the animal facility and killed at varying ages up to 12 months for analysis of lung phospholipid content. All experimental animal procedures were approved by the University of Pennsylvania Institutional Animal Care and Use Committee.

Alveolar type 2 epithelial cells were isolated from mouse lungs by a previously described procedure using endotracheal dispase for lung digestion (16). Cell isolates were seeded onto type I collagen-coated 35 mm dishes in Ham's F-12 culture medium supplemented with 15 mM HEPES, 0.8 mM $CaCl_2$, 0.25% BSA, 5 μg/ml insulin, 5 μg/ml transferrin, 5 ng/ml sodium selenite, and 2% mouse serum and incubated for 24 h before study. The isolated cells at 24 h were 95% type 2 alveolar epithelial cells, as judged by cytokeratin staining and the presence of Nile Red-positive vacuoles.

Morphology

Mouse lungs were fixed with 2.5% glutaraldehyde plus 4% paraformaldehyde by perfusion through the pulmonary artery followed by endotracheal inflation and immersion in fixative for 4 h at 4°C. Lungs were postfixed for 1 h with 2% OsO_4 followed by 30 min with 2% uranyl acetate, then dehydrated with graded acetone and embedded in Epson 812, which was polymerized at 55°C for 48 h. For light microscopy, 500 nm thick sections were cut and stained with toluidine blue. For examination with a JEOL 100 electron microscope, 70 nm sections were cut and counterstained for 10 min with 2% uranyl acetate and for 10 min with lead citrate.

Preparation of liposomes

Unilamellar liposomes were prepared with the composition (mole fraction) 0.5 DPPC, 0.25 egg phosphatidylcholine (PC), 0.15 cholesterol, and 0.10 phosphatidylglycerol to reflect the approximate composition of lung surfactant (6, 17). Liposomes contained trace radiolabeled DPPC with [^{3}H-*methyl*]choline label for perfused lung studies or [9,10-^{3}H]palmitate label for PLA_2 assays. In some preparations, MJ33 was added at 3 mol/100 mol lipid. Unilamellar liposomes (mean diameter, 120 nm) were prepared by evaporating the mixture of lipids under N_2 to dryness, resuspending the evaporated film in PBS with vigorous mixing, freezing and thawing three times by alternating exposure to liquid N_2 and a 50°C water bath, and then extruding at 50°C for 10 cycles through a 100 μm pore size filter. Liposomes were stored overnight at 4°C and then centrifuged to remove large aggregates before use.

Isolation of lung fractions

To isolate subcellular fractions, lungs were lavaged through the trachea five times with 1 ml of normal saline. The material obtained is called the bronchoalveolar lavage fluid (BALF). Lung surfactant was isolated from the BALF using a NaCl gradient (17). Lamellar bodies were isolated from homogenates of postlavage lungs by upward flotation using a sucrose density gradient (17). To isolate alveolar macrophages, the BALF was centrifuged at 100 *g* for 10 min. The resulting pellet was resuspended in medium and incubated for 1 h at room temperature on 35 mm plastic dishes. The dishes were washed three times to remove nonadherent cells, and the adherent macrophages were scraped and disrupted by sonication (6). Protein was measured by the Coomassie Blue binding assay (Bio-Rad, Richmond, CA) using bovine γ globulin as the standard.

PLA_2 activity

PLA_2 activity was measured in lung homogenates and lamellar bodies as described previously (6, 17). Activity was measured at pH 4.0 in 40 mM sodium acetate and 5 mM EDTA buffer and at pH 8.5 in 50 mM Tris-HCl, 1 mM EGTA, and 10 mM $CaCl_2$ buffer using a liposome-based assay and radiochemical detection. The substrate was the standard surfactant-like liposomes labeled with 1-palmitoyl, 2-[9,10-^{3}H]palmitoyl, *sn*-3 glycerophosphorylcholine ([^{3}H]DPPC) at a specific activity of 2 mCi/mmol DPPC. Assays were carried out in the presence and absence of 3 mol% MJ33 added to liposomes. The reaction was stopped by the addition of $CHCl_3/CH_3OH$ (1:2, v/v), lipids were extracted, components were separated by a two-step TLC procedure using hexane-ether-acetic acid, and the free fatty acid spot was scraped and assayed for dpm (3).

Separation of phospholipid classes

Lipids were extracted using the Bligh and Dyer (18) procedure to obtain lipid and aqueous fractions. Lipid fractions were separated further into individual classes by TLC on silica gel using a solvent system of chloroform/methanol/NH_4OH/water (65:35:2.5:2.5) (19). The lipid spots were visualized by brief exposure to I_2 vapors and then scraped for analysis of lipid phosphorous (20) or determination of dpm. Authentic standards were cochromatographed for identification of individual lipids.

The disaturated phosphatidylcholine (DSPC) fraction was separated from total PC on a neutral alumina column after treatment of lipids with OsO_4 (21). This method measures DSPC (i.e., PC in which both fatty acids are saturated). In this article, we refer to DSPC when the osmication method was used for identification and DPPC for the authentic phospholipid.

Lung perfusion

Isolated lung perfusion was carried out as described previously (22). Mice were anesthetized with 60 mg/kg pentobarbital intraperitoneally. The abdomen and chest of the anesthetized and continuously ventilated mouse were incised, and the lungs were cleared of blood by perfusion with Krebs Ringer bicarbonate solution supplemented with 3% fatty acid-free BSA and 10 mM glucose. The heart was trimmed away, and the lungs were removed from the thorax and placed in a temperature-controlled (37°C) incubation chamber. Lungs were ventilated continuously at 60 cycles/min with 0.3 ml tidal volume of 5% CO_2 in air and perfused with recirculating Krebs Ringer bicarbonate at 2 ml/min.

Uptake and degradation of DPPC

Uptake of DPPC in liposomes by the isolated lung was studied according to a previously described protocol (6, 17, 23). Liposomes were labeled with ^{3}H-*methyl* in the choline moiety of DPPC. Unilamellar liposomes (20 nmol of total lipid in 20 μl of saline) were instilled into the trachea of the anesthetized mouse at the approximate level of the carina. The lungs were then removed from the chest and either immediately homogenized (~5 min after liposome instillation) or perfused for 2 h as described above. At the end of perfusion, lungs were homogenized and an aliquot of the homogenate and recirculating perfusate was analyzed for dpm. The remaining homogenate was then analyzed for dpm in the aqueous fraction and lipid classes as described above. The specific activity of alveolar [^{3}H]DPPC was calculated from the injected dose and the measured alveolar DPPC pool size. Uptake of DPPC was calculated from the total lung (plus perfusate) dpm and the alveolar DPPC specific activity. Recovery of dpm in the perfusate was <2% of total recovered dpm and has been shown previously to represent dpm in free choline (24). Degradation was calculated from the dpm recovered in the sum of the aqueous PC, lysoPC, and unsaturated PC fractions and expressed as a percentage of total recovery. The sum of degradation products expressed this way equals 100% minus the percentage of dpm recovered in the DSPC fraction. This calculation cannot account for DSPC that has been resynthesized from [^{3}H]lysoPC plus saturated fatty acid and thus underestimates actual PLA_2 activity.

To study metabolism in isolated type 2 cells, cells adherent to the dish after 24 h of culture were incubated with [^{3}H]DPPC-labeled unilamellar liposomes for 3 h (6). Cells were then extracted and analyzed for dpm in lipid classes as described for the perfused lung.

Synthesis of DSPC

Synthesis of DSPC was evaluated using a protocol described previously for the rat lung (23). Liposomes (20 nmol of total lipid) without radioactive label but with or without 3 mol% MJ33 were instilled endotracheally as described above. The liposomes were used as a means to deliver MJ33 to the lung epithelium. One hour later, mice were injected with a mixture of [^{3}H-*methyl*]choline (10 μCi) and [1-^{14}C]palmitate (1 μCi) through the tail vein. After 24 h, the mice were killed by exsanguination under anesthesia. Lungs were lavaged to obtain the surfactant fraction, and the postlavage lungs were used to isolate lamellar bodies. These fractions were assayed for incorporation of the ^{14}C and ^{3}H labels into DSPC.

Statistics

Results are presented as means ± SEM. Statistical significance was determined by *t*-test after one-way ANOVA using SigmaStat (Jandel Scientific, San Rafael, CA). The level of statistical significance was taken as $P < 0.05$.

RESULTS

As reported previously, Prdx6$^{-/-}$ mice grew and reproduced normally. Body weight at 9–11 weeks (~24 g) was similar for wild-type and knockout mice. Light microscopy indicated no difference between the wild-type and Prdx6$^{-/-}$ mouse lungs examined at 2 and 6 months of age (data not shown). Lung tissue of the two species also was similar on examination at the ultrastructural level (**Fig. 1**). The type 2 cells of control and gene-targeted lungs showed similar morphology, with no qualitative differences of lamellar body ultrastructure, size, or distribution. Alveolar macrophages (shown at low magnification in Fig. 1) appeared similar at higher magnification (data not shown) in Prdx6$^{-/-}$ and wild-type control mice.

We have shown previously that Prdx6 mRNA by real-time PCR and protein content by immunoblot analysis are absent in lungs of Prdx6$^{-/-}$ mice and are decreased in heterozygotes by 50% compared with wild-type animals (13). PLA_2 activity was measured in the lung homogenate and in lamellar bodies and alveolar macrophages isolated from the lung. Activity measured at acidic pH in Ca^{2+}-free buffer and in the presence of MJ33 is identified as $aiPLA_2$ activity. For all three sources of enzyme, activity was inhibited by ~80% in the presence of 3 mol% MJ33 (data not

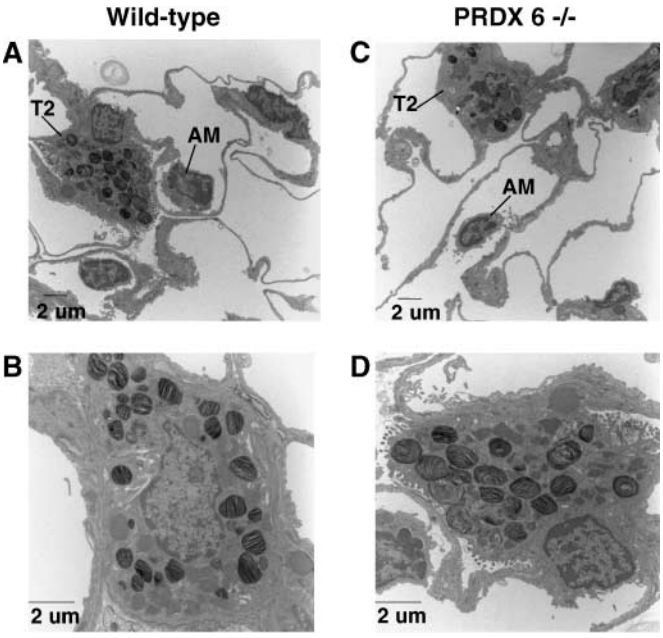

Fig. 1. Ultrastructure of lung tissue from wild-type (C57BL/6) and peroxiredoxin 6 knockout (Prdx6$^{-/-}$) mice. Lungs were fixed by endotracheal inflation. A, C: Low-magnification images of alveolar septae. An alveolar epithelial type 2 cell (T2) and an alveolar macrophage (AM) are indicated. B, D: Higher magnification of in situ type 2 cells.

TABLE 1. Ca^{2+}-independent, MJ33-sensitive PLA_2 activity at pH 4 of mouse lung homogenate and lamellar bodies

Mouse	PLA_2 Activity		
	Lung Homogenate	Lung Lamellar Bodies	Alveolar Macrophages
	nmol in 1 h/mg protein		
Wild type	7.1 ± 0.4	23.3 ± 1.7	3.6 ± 0.05
$Prdx6^{+/-}$	3.8 ± 0.4[a]	ND	ND
$Prdx6^{-/-}$	0.19 ± 0.02[a]	0.88 ± 0.04[a]	0.37 ± 0.06[a]

ND, not determined; PLA_2, phospholipase A_2; $Prdx6^{-/-}$, peroxiredoxin 6 knockout. Values are means ± SEM for n = 3. PLA_2 activity was measured at pH 4 in calcium-free buffer with 3 mol% MJ33 in liposomes.

[a] $P < 0.05$ versus the corresponding value for the wild type (C57BL/6).

shown). Activity in the wild-type mouse lung homogenate expressed on a protein basis (**Table 1**) was approximately one-half of the values that we reported previously for the rat lung (25). Wild-type mice showed ~3-fold enrichment in $aiPLA_2$ activity in lamellar bodies compared with lung homogenate, whereas activity in alveolar macrophages was ~50% less. Only slight activity that was not significantly different from background was detected for lung homogenate from the gene-targeted mice, whereas the activity of the heterozygous mouse lung was approximately midway between that for the wild-type and knockout lungs (Table 1). $aiPLA_2$ activity in lamellar bodies from the $Prdx6^{-/-}$ mouse was ~4% of the corresponding wild-type activity, and that in $Prdx6^{-/-}$ alveolar macrophages was 10% of wild-type activity (Table 1). Ca^{2+}-dependent PLA_2 activity of the lung homogenate measured at pH 8.5 was 9.5 ± 0.4 nmol in 1 h/mg protein in wild-type and 9.4 ± 0.2 nmol in 1 h/mg protein in $Prdx6^{-/-}$ lung homogenate (n = 3). There was no effect of MJ33 on PLA_2 activity at pH 8.5 in either wild-type or knockout mouse lung homogenate.

We measured phospholipid composition in the BALF, the lung homogenate, and lung lamellar bodies (**Table 2**). The major phospholipid in all three fractions is PC, which represents >75% of total phospholipid in the BALF and lamellar bodies and ~40% of total phospholipid in lung homogenate of wild-type mice; DSPC was approximately two-thirds of total PC. There was no significant difference in the phospholipid composition of C57BL/6 and 129SvJ mice (Table 1). In $Prdx6^{-/-}$ lungs, total phospholipid, PC, and DSPC were all increased significantly compared with wild-type lungs in the BALF, lung homogenate, and lamellar bodies. The increase in phospholipid fractions in knockout mice ranged from 25% to 77% greater than in the wild type. The percentage of phospholipid accounted for by PC and the percentage of PC accounted for by DSPC were similar in wild-type and knockout animals. These results indicate a proportionate increase in all surfactant phospholipid components in the gene-targeted mouse. The phospholipid contents of BALF and lung homogenate also were measured as a function of mouse age. The lung content of total phospholipid, PC, and DSPC in wild-type lungs was not changed significantly between ages 10 and 40 weeks when normalized to body weight (for BALF) or milligrams of protein (for lung homogenate) (**Fig. 2**). However, lungs from $Prdx6^{-/-}$ mice between 4 and 48 weeks of age showed a progressive increase in phospholipid content (Fig. 2). The increase was similar in degree for total phospholipids, PC, and DSPC.

Uptake of DPPC by the isolated perfused lung was measured at 2 h after instillation of mixed unilamellar liposomes into the alveolar spaces. Uptake was similar for wild-type and $Prdx6^{-/-}$ mouse lungs (**Table 3**). Values for uptake were calculated from specific activities of the substrate based on the measured PC content of the BALF, so that differences in alveolar phospholipid pool size were taken into account. The $aiPLA_2$ inhibitor MJ33 had no effect on lung uptake of DPPC in either wild-type or gene-targeted lungs (data not shown).

Degradation of DPPC that had been internalized by the lung during the 2 h perfusion period was evaluated under basal conditions and in the presence of MJ33. In wild-type lungs, total degradation was 27% of internalized DPPC and was decreased by nearly one-half in the presence of MJ33 (**Fig. 3**). In $Prdx6^{-/-}$ lungs, total lung degradation of DPPC also was decreased by ~50% compared with wild-type lungs (Fig. 3). Unlike the wild type, the presence of MJ33 had no effect on degradation in $Prdx6^{-/-}$ mice (Fig. 3). Recovery of dpm was determined in the DPPC, unsaturated PC, lysoPC, and aqueous fractions (**Table 4**). We have shown previously after incubation of rat lung and lung cells with [^{3}H]choline-labeled DPPC that dpm in the aqueous fraction represents labeled glycerophosphorylcholine, choline phosphate, CDP-choline, and free choline (26, 27). Dpm in the unsaturated PC fraction represents PC containing an unsaturated fatty acid, generally in the *sn*-2 position, and is presumably generated from labeled lysoPC in what has been called the reacylation path-

TABLE 2. Phospholipid content in mouse lung fractions

Phospholipid	BALF			Lung			Lamellar Bodies	
	C57BL/6	129Sv/J	$Prdx6^{-/-}$	C57BL/6	129Sv/J	$Prdx6^{-/-}$	C57BL/6	$Prdx6^{-/-}$
	μg/g body weight			*μg/mg protein*			*μg/μg protein*	
PL	8.8 ± 0.1	8.7 ± 0.3	13.1 ± 0.3[a]	83.3 ± 3.0	84.9 ± 5.0	121.1 ± 3.0[a]	9.2 ± 0.02	12.1 ± 0.4[a]
PC	6.7 ± 0.2	6.7 ± 0.4	10.6 ± 0.4[a]	31.1 ± 1.0	29.7 ± 0.7	53.7 ± 1.1[a]	7.0 ± 0.3	9.0 ± 0.2[a]
DSPC	4.3 ± 0.1	4.6 ± 0.3	6.9 ± 0.3[a]	20.4 ± 0.7	18.4 ± 0.4	32.6 ± 0.2[a]	3.9 ± 0.2	4.9 ± 0.1[a]

BALF, bronchoalveolar lavage fluid; DSPC, disaturated phosphatidylcholine; PC, phosphatidylcholine; PL, total phospholipid. Values are means ± SEM for n = 3 mice (24 ± 0.6 g body weight) in each group. Lung indicates whole lung homogenate after lavage and cleared of blood.

[a] $P < 0.05$ versus the corresponding value for the wild type (C57BL/6).

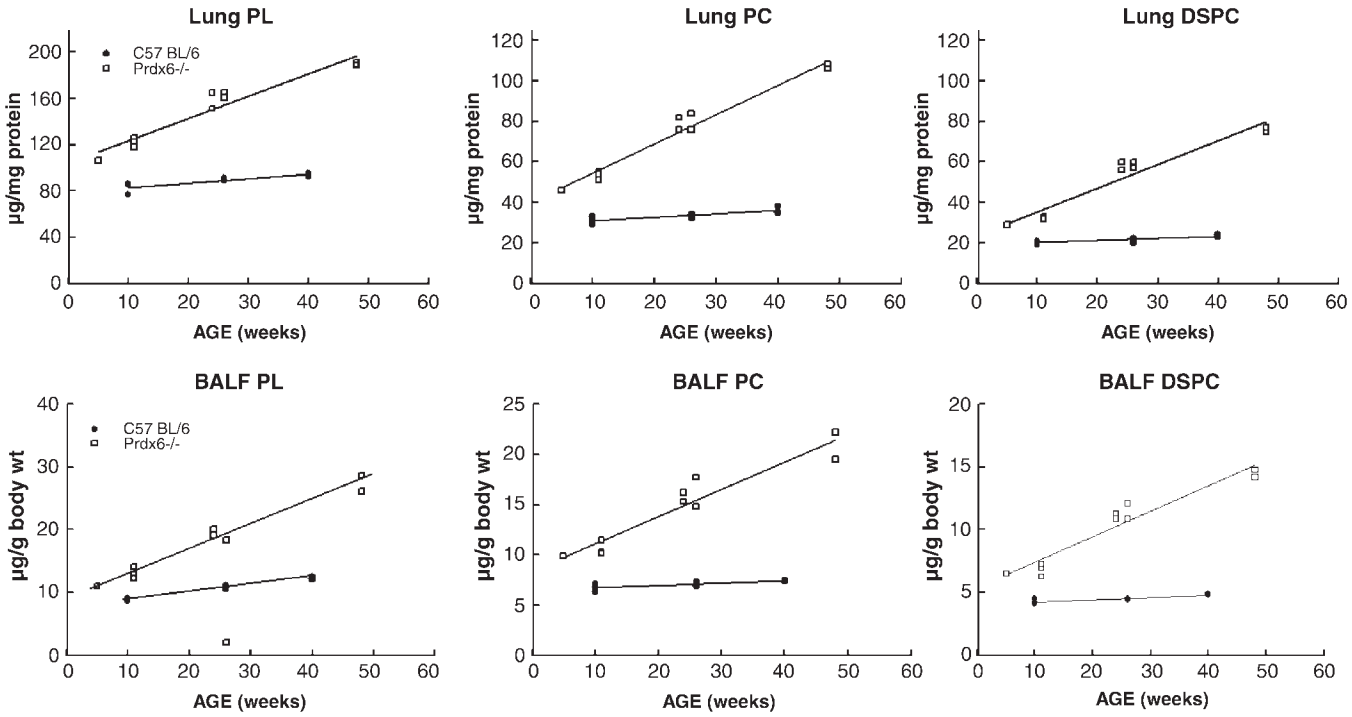

Fig. 2. Change in lung and bronchoalveolar lavage fluid (BALF) phospholipid content with age (in weeks) in wild-type (C57BL6) and Prdx6$^{-/-}$ mice. The panels show total phospholipid (PL), phosphatidylcholine (PC), and disaturated phosphatidylcholine (DSPC) in the lung homogenate (top row) and BALF (bottom row). The lipid measurements are normalized to lung protein for the lung homogenate and to body weight for BALF. The plotted values for 10–11 weeks of age are the same results used to calculate means ± SEM for C57BL/6 and Prdx6$^{-/-}$ mice in Table 2. The lines represent linear least mean square regression fits (SigmaStat; Jandel Scientific).

way of PC synthesis (1). The presence of MJ33 resulted in significantly decreased recovery of dpm in lysoPC and unsaturated PC fractions, whereas recovery in the aqueous fraction was decreased only slightly (Table 4). These results are compatible with the inhibition of PLA_2-mediated DPPC degradation. Lungs from Prdx6$^{-/-}$ mice compared with wild-type mice also showed decreased recovery of dpm in lysoPC and unsaturated PC fractions, with only a small (not significant) difference for the aqueous fraction, a pattern similar to the observed effect of MJ33 in wild-type mice.

Uptake and degradation of [^{3}H]DPPC also were studied in lung type 2 epithelial alveolar cells in primary culture. Similar to the results obtained with the isolated perfused lung, DPPC uptake was approximately the same for cells from wild-type and Prdx6$^{-/-}$ lungs (Table 3), but degradation in Prdx6$^{-/-}$ cells was significantly lower (**Fig. 4**). As with the lung, there was a large decrease in dpm recovery in the unsaturated PC fraction in granular pneumocytes from the Prdx6$^{-/-}$ mice, whereas dpm recoveries in the aqueous and lysoPC fractions were not changed significantly (Fig. 4).

DSPC synthesis was studied after simultaneous intravenous injection of [^{3}H]choline and [^{14}C]palmitate. The rationale for use of the two labels is that choline represents incorporation primarily through the de novo pathway for DSPC synthesis, whereas incorporation of palmitate reflects

TABLE 3. Uptake of [^{3}H]DPPC in mixed unilamellar liposomes

Mouse	Perfused Lung	Isolated Type 2 Cells
	nmol in 2 h/lung	*nmol in 3 h/mg protein*
Wild type	7.7 ± 0.5	2.4 ± 0.4
Prdx6$^{-/-}$	7.0 ± 0.7	2.9 ± 0.4

DPPC, dipalmitoylphosphatidylcholine. Values represent net uptake (5 min baseline value subtracted) and are means ± SEM for n = 3. For lung, the specific activity of DPPC was calculated from the DPPC content in the BALF and the instilled [^{3}H]DPPC.

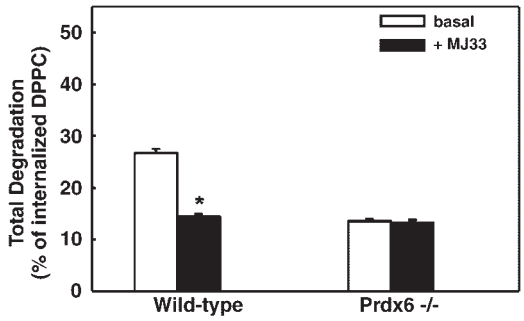

Fig. 3. Degradation of internalized ^{3}H-labeled dipalmitoylphosphatidylcholine ([^{3}H]DPPC) by isolated, perfused wild-type (C57BL/6) and Prdx6$^{-/-}$ mouse lungs. Degradation was measured at 2 h after endotracheal installation of [^{3}H]DPPC. Total degradation is calculated from the dpm in DSPC as a percentage of total counts recovered (DSPC, unsaturated PC, lysoPC, and the aqueous fraction in lungs plus perfusate). Basal conditions represent perfused lungs with no additions. Results are means ± SEM for n = 3 for each condition. * $P < 0.05$ versus basal.

TABLE 4. Degradation of internalized DPPC: recovery of dpm in lipid fractions

Fraction	Wild Type		Prdx6$^{-/-}$	
	Basal	+MJ33	Basal	+MJ33
	% of total recovery			
LysoPC	2.0 ± 0.1	0.4 ± 0.1[a]	0.5 ± 0.1[b]	0.5 ± 0.1
Unsaturated PC	15.9 ± 0.9	6.8 ± 0.2[a]	5.8 ± 0.3[b]	5.7 ± 0.3
Aqueous	8.7 ± 0.3	7.3 ± 0.1[a]	7.7 ± 0.4	7.2 ± 0.3

Lungs were perfused for 2 h after liposome instillation. Lung extracts were separated into aqueous and lipid classes and analyzed for radioactivity. Aqueous fraction indicates aqueous soluble dpm in lungs plus perfusate. Values are means ± SEM for n = 3.

[a] $P < 0.05$ versus the corresponding basal value.

[b] $P < 0.05$ versus the corresponding value for the wild type (C57BL/6).

in addition the reacylation pathway (1). Incorporation of substrate was measured both in lamellar bodies isolated from the lung homogenate and in surfactant isolated from the BALF. Incorporation is expressed as dpm per nanomole of DSPC, because the intracellular pool sizes for the precursor substrates are not known. The incorporation (specific activity) of choline into lamellar body DSPC was approximately twice that observed in surfactant DSPC in wild-type lungs (**Fig. 5A**), compatible with lamellar bodies as the storage organelle for surfactant secretion. There was a slight decrease of choline incorporation in both lamellar body and surfactant DSPC in the presence of MJ33 and a similar small decrease of incorporation in Prdx6$^{-/-}$ lungs compared with wild-type lungs (Fig. 5A). By contrast, incorporation of palmitate in Prdx6$^{-/-}$ lungs showed a 73% decrease in lamellar body DSPC and a 54% decrease in surfactant DSPC compared with the wild type (Fig. 5B). MJ33 depressed palmitate incorporation in wild-type lungs to the same extent as did deletion of the Prdx6 gene (Fig. 5B). Treatment of Prdx6$^{-/-}$ lungs with

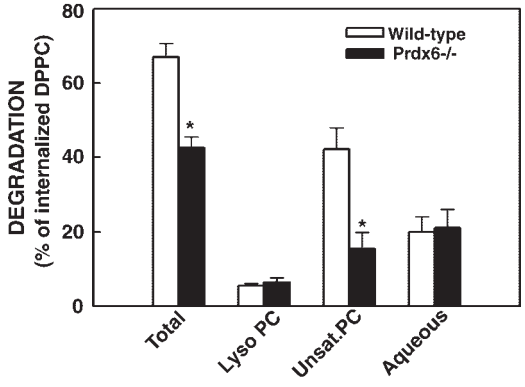

Fig. 4. Degradation of [^{3}H]DPPC by isolated type 2 alveolar epithelial cells from wild-type (C57BL/6) and Prdx6$^{-/-}$ lungs in primary culture. Cells at 24 h after isolation were incubated with [^{3}H]DPPC-labeled unilamellar liposomes for 3 h. Total degradation was measured as a percentage of recovered dpm in DSPC as described for Fig. 3. Recovery of dpm also was measured in the lysoPC, unsaturated PC, and aqueous fractions. Results are means ± SEM for n = 3 for each condition. * $P < 0.05$ versus the wild type.

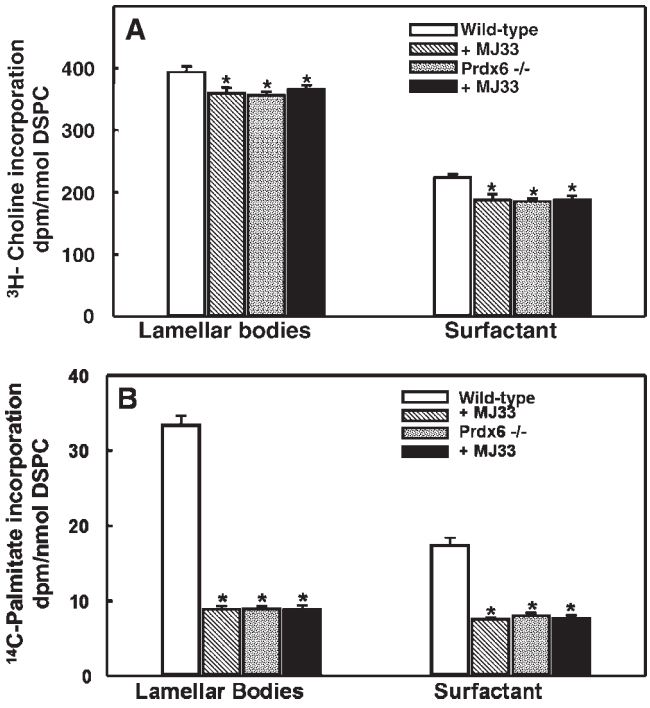

Fig. 5. Incorporation of radiolabeled substrate into DSPC of lung lamellar bodies and surfactant fractions isolated from wild-type (C57BL/6) and Prdx6$^{-/-}$ lungs. Liposomes with or without 3 mol% MJ33 were instilled into the lungs by endotracheal instillation, and [^{3}H]choline and [^{14}C]palmitate were injected into the tail vein 1 h later. At 24 h, surfactant was isolated from the BALF, and lamellar bodies were isolated from the lung homogenate. The DSPC fraction was isolated from surfactant and lamellar bodies and analyzed for dpm and phospholipid phosphorus. A: Incorporation of [^{3}H]choline into DSPC. B: Incorporation of [^{14}C]palmitate into DSPC. Results are means ± SEM for n = 3 for each condition. * $P < 0.05$ versus the wild type.

MJ33 had no effect on the incorporation of substrates into DSPC (Fig. 5A, B). Thus, MJ33 and targeted deletion of the Prdx6 gene had similar effects on DSPC synthesis in the lungs.

DISCUSSION

We have shown previously that MJ33, a PLA_2 inhibitor, markedly inhibits the degradation of DPPC after its internalization by lung type 2 alveolar epithelial cells either in situ or in primary culture (3, 6). With an in vitro assay, MJ33 inhibited PLA_2 activity that was Ca^{2+}-independent and maximal at pH 4 but had no effect on Ca^2-dependent PLA_2 activity assayed at pH 8 (3, 6). Based on this finding, we proposed that the degradation of DPPC in the lung epithelium was attributable in large part to the activity of a lysosomal type of PLA_2. However, MJ33 is known to inhibit other PLA_2 activities (7, 28), so the result of these inhibitor studies could not be considered definitive. In the present study, we have continued the evaluation of the effects of aiPLA$_2$ on lung DPPC metabolism using mice lacking Prdx6 generated by targeting of the Prdx6 gene (13).

Prdx6 is a bifunctional enzyme, and assay of the protein isolated from lungs or generated by recombinant technology has indicated the presence of aiPLA$_2$ activity that is inhibited by MJ33 (8, 12, 25, 29). Furthermore, lungs of the homozygous Prdx6 gene-targeted animals showed essentially absent aiPLA$_2$ activity. Thus, this mouse is suitable to study the role of aiPLA$_2$ in lung surfactant phospholipid metabolism.

DPPC metabolism was studied using radiolabeled DPPC delivered to lung cells in mixed unilamellar liposomes. DPPC metabolism was markedly altered in the gene-targeted mice, with a significant decrease in total degradation of DPPC measured over a 2 h period in the lung or a 3 h period in isolated cells. Analysis of degradation products in the lung showed decreased radiolabel in lysoPC, the primary product of aiPLA$_2$ activity. LysoPC normally is either degraded further or reacylated (the so-called reacylation pathway) to regenerate PC (1). As we have shown previously, the reacylation pathway generates unsaturated PC in lung epithelial cells (6, 17); regeneration of labeled DPPC presumably also occurs, but this cannot be differentiated from the original substrate. The amount of label present in unsaturated PC was reduced markedly compared with the wild type in Prdx6$^{-/-}$ lungs and type 2 cells isolated from Prdx6$^{-/-}$ mice. Radiolabel in unsaturated PC must arise either through reacylation or de novo synthesis, because all of the label originally was in the disaturated species, DPPC. Because de novo synthesis was relatively little affected by Prdx6 knockout, decreased label in unsaturated PC reflects decreased reacylation. This result is compatible with the decreased generation of labeled lysoPC in the gene-targeted animals attributable to the absence of aiPLA$_2$ activity. The third sink for the [^{3}H]choline moiety of DPPC after degradation is in aqueous soluble degradation products (26, 27). These products arise through the activity of phospholipases C and D on DPPC to generate labeled free choline or choline phosphate or by the degradation of [^{3}H]lysoPC by lysophospholipases and phosphatases. The generation of aqueous soluble metabolic products was not significantly different in Prdx6$^{-/-}$ mice compared with wild-type mice, indicating that the altered metabolism was specific for PLA$_2$ activity.

Altered PLA$_2$ activity also was reflected in results for substrate incorporation into DPPC after intravenous injection of radiolabeled choline and palmitate. Incorporation of free choline reflects primarily the de novo pathway for DPPC synthesis, in which choline is converted to CDP-choline and combines with diacylglycerol. On the other hand, palmitate incorporation reflects both the de novo and the reacylation pathways (17). As described above, the reacylation pathway requires PLA$_2$ activity to generate the lysoPC as an acceptor for acyltransferase-mediated transfer of fatty acid. The gene-targeted mice had only a minimal decrease in choline incorporation into DSPC, indicating that the de novo pathway was largely intact. Therefore, the activity of this pathway, coupled with a decreased rate of degradation, could maintain the surfactant DSPC pool. However, labeled palmitate incorporation into DSPC was decreased markedly, compatible with decreased lysoPC availability attributable to the loss of PLA$_2$ activity. The changes in DPPC degradation and DSPC synthesis in knockout mice were similar to the effects of MJ33 in wild-type mice. Furthermore, the addition of MJ33 to lung homogenates from Prdx6$^{-/-}$ mice had no additional effect, indicating that there is no other PLA$_2$ enzyme in the lung with significant MJ33-sensitive activity. These results indicate that Prdx6 deletion and MJ33 have similar effects and that the effect of MJ33 on lung DPPC metabolism is the result of its inhibition of aiPLA$_2$ activity.

The subcellular site of DPPC degradation after its internalization by alveolar type 2 cells has been identified as the lysosomes (5, 30). Rat lung subcellular fractionation studies have indicated the presence of Prdx6 (29) protein and aiPLA$_2$ activity (6) in the lysosomal fraction as well as in lamellar bodies, which are considered to be modified lysosomes. Thus, lysoPC would be generated in those organelles associated with aiPLA$_2$ activity. On the other hand, the site of lysoPC reacylation is presumed to be the endoplasmic reticulum, where the required acyltransferase has been identified (31). Thus, the present results suggest cooperativity between the lysosomes and the endoplasmic reticulum for the synthesis of DPPC by the reacylation pathway. This interaction has been noted previously during studies of the effect of lysosomatrophic agents (chloroquine, quinacrine) on DPPC synthesis by type 2 pneumocytes (32–34). The mechanisms for the transfer of lysoPC between the lysosomal and the endoplasmic reticulum compartments have not been described.

The designation PLA$_2$ represents a broad family of enzymes that can be characterized as intracellular or extracellular forms (35–39). The extracellular forms are secreted enzymes that are of low molecular mass (~14 kDa) and require high Ca^{2+} (~1 mM) for maximal activity. These enzymes are components of snake and bee venoms and also are found in gastrointestinal secretions and inflammatory exudates. Intracellular PLA$_2$s have been described more recently. These enzymes are larger than the secreted forms, although their size varies over a wide range. The Ca^{2+} requirement for some is in the low micromolar range, consistent with the usual intracellular concentration of this ion, whereas others are Ca^{2+}-independent (36). These intracellular enzymes have a broad role in phospholipid metabolism, including phospholipid synthesis and remodeling and the provision of arachidonic acid for eicosanoid generation (39, 40). The intracellular enzymes generally have a pH optimum in the slightly alkaline range, consistent with their cellular cytoplasmic localization. Secreted and intracellular PLA$_2$ enzymes that have been identified in lung tissue include groups II, IV, V, and X PLA$_2$ (41–43).

In addition to secreted and intracellular cytoplasmic PLA$_2$s, assay of lungs and some other tissues has revealed PLA$_2$ activity that is maximal at acidic pH and is Ca^{2+}-independent (3, 44, 45). Although its subcellular localization is not known definitively, activity has been attributed to the lysosome as a degradative organelle with an acidic pH. As described above, this lysosomal-type activity in the

lung is inhibited by MJ33 (3, 17). PLA_2 activity that is Ca^{2+}-independent, maximal at pH 4, and inhibited by MJ33 has been demonstrated for Prdx6 isolated from lungs (25, 29) and polymorphonuclear leukocytes (46) and for recombinant Prdx6 (12, 25). Prdx6 mRNA and protein are widely distributed throughout mammalian tissues, but content in the lung is greater than in other major organs (25, 47). Lung subcellular fractionation studies indicated localization of Prdx6 to the lamellar body and the lysosomal fractions, both acidic organelles (48) and the cytosol (25). The latter may represent the glutathione peroxidase activity of Prdx6 (9–11). The gene-targeted mice show a 97% decrease of the $aiPLA_2$ activity compared with wild-type mice, indicating that Prdx6 accounts for most of the lysosomal-type activity that is present in lung homogenate.

Recently, a second lysosomal PLA_2, originally called acylceramide synthase, was isolated from bovine brain, and its molecular sequence has been provided (49). Acylceramide synthase (also called $LPLA_2$) can hydrolyze DPPC. Although $LPLA_2$ and the enzymatic activity were reported to be sensitive to MJ33, 50% inhibition required ~20 mol% of the inhibitor (28) compared with 90% inhibition at 3 mol% for recombinant $aiPLA_2$ (12). Because lung homogenate PLA_2 activity at pH 4 was 97% inhibited by 3 mol% MJ33, this effect was most likely attributable mainly to $aiPLA_2$ rather than $LPLA_2$. $LPLA_2$ is highly enriched in lung alveolar macrophages, but the mRNA and activity are very low in lung tissue (28). Thus, this enzyme is unlikely to be involved in normal lung DPPC turnover, because the alveolar macrophage normally accounts for a relatively minor fraction of lung surfactant phospholipid degradation and does not participate in lung surfactant PC remodeling (2, 4, 50). The present results with alveolar macrophages from $Prdx6^{-/-}$ mice showed very low residual activity, indicating that $LPLA_2$ could account for less than 10% of total $aiPLA_2$ activity in those cells. The present studies used 3 mol% MJ33, which caused >40% inhibition of lung DPPC metabolism in wild-type lungs. At this concentration of MJ33, $LPLA_2$ is inhibited by ~10% (28), whereas $aiPLA_2$ is inhibited by 90% (12). This comparison provides additional evidence that $LPLA_2$ did not contribute significantly to the observed effects.

The present results with $Prdx6^{-/-}$ mice indicate that this enzyme is responsible for ~40% of lung degradation of internalized DPPC. MJ33 in wild-type mouse lung showed inhibition of DPPC degradation similar in degree to the knockout mouse. Although we have not studied alternative pathways for DPPC degradation in mouse lungs, we have evaluated rat lungs and cultured rat alveolar type 2 cells. Approximately 20% of lung DPPC degradation is attributable to PLA_2 enzymes that are insensitive to MJ33 but inhibited by *p*-bromophenacylbromide (6). The possible enzymes involved include groups II, V, and X PLA_2s, which have been identified in lung tissue (41). The activity of these enzymes is reflected by the assay of lung homogenate at pH 8.5 in the presence of Ca^{2+}. This activity was not induced in $Prdx6^{-/-}$ lungs. Another 30% of DPPC degradation in the rat lung occurs via phospholipase C or D (3). These latter enzymes may be largely responsible for the recovery of label from DPPC in the aqueous fraction. In the present experiments, this latter fraction represented 33% of total metabolites. The dpm recovered in the aqueous fraction with wild-type and knockout lungs was similar, suggesting that phospholipase C or D is not induced in $Prdx6^{-/-}$ mouse lung. In all, enzymes other than Prdx6 are responsible for 50–60% of lung DPPC degradation. However, these other enzymes did not fully compensate for the absence of Prdx6 (i.e., $aiPLA_2$ activity), because there was a progressive time-dependent accumulation of lung and alveolar phospholipid in the knockout mouse. Also, these alternative pathways are apparently unable to supply sufficient lysoPC substrate to maintain normal rates of DPPC synthesis by the reacylation pathway, as indicated by the very low rates of palmitate incorporation into DPPC in the knockout mouse. A mechanism that may have compensated, in part, for the loss of $aiPLA_2$ activity in the knockout lungs is an increased rate of DPPC recycling without degradation. It is known that the balance between recycling and degradation can depend on the physiological state of the lung. For example, recycling of DPPC accounts for a much higher percentage of DPPC turnover in the neonatal rat lung compared with the adult lung (2, 51). Thus, the activity of other phospholipases, increased surfactant DPPC recycling, and modulation of the rate of synthesis all could play a role in ameliorating the effects of decreased degradation via $aiPLA_2$ activity in the $Prdx6^{-/-}$ mouse lung.

In summary, the present studies show that mice with a targeted deletion of the Prdx6 gene have the phenotype of increased lung phospholipid content. Associated biochemical defects include altered lung phospholipid metabolism with decreased degradation of DPPC after its internalization from the alveolar space and decreased DPPC synthesis through the reacylation pathway. The degree of metabolic alteration in the $Prdx6^{-/-}$ mouse lungs is similar to the effect of MJ33 in wild-type lungs. These results indicate that MJ33 functions as an inhibitor of $aiPLA_2$ and that Prdx6 has PLA_2 activity that has a major role in lung surfactant phospholipid metabolism.

The authors thank Dr. Mahendra Jain for encouragement and advice, Dr. Sandy Bates for advice about cell isolation, Tea Shuvaev, Kevin Yu, Lu Lu, and Jain-Qin Tao for technical assistance, and Jennifer Rossi for typing the manuscript. This work was supported by Grant HL-19737 from the National Institutes of Health.

REFERENCES

1. Batenburg, J. J., and H. P. Haagsman. 1998. The lipids of pulmonary surfactant: dynamics and interactions with proteins. *Prog. Lipid Res.* **37:** 235–276.
2. Fisher, A. B. 1998. Surfactant Catabolism and Recycling. Landes Bioscience, Austin, TX.
3. Fisher, A. B., C. Dodia, A. Chander, and M. Jain. 1992. A competitive inhibitor of phospholipase A2 decreases surfactant phosphatidylcholine degradation by the rat lung. *Biochem. J.* **288:** 407–411.
4. Rider, E. D., M. Ikegami, and A. H. Jobe. 1992. Localization of alveolar surfactant clearance in rabbit lung cells. *Am. J. Physiol.* **263:** L201–L209.

5. Rider, E. D., M. Ikegami, K. E. Pinkerton, J. L. Peake, and A. H. Jobe. 2000. Lysosomes from rabbit type II cells catabolize surfactant lipids. *Am. J. Physiol. Lung Cell. Mol. Physiol.* **278:** L68–L74.
6. Fisher, A. B., and C. Dodia. 1996. Role of phospholipase A2 enzymes in degradation of dipalmitoylphosphatidylcholine by granular pneumocytes. *J. Lipid Res.* **37:** 1057–1064.
7. Jain, M. K., B. Z. Yu, J. Rogers, G. N. Ranadive, and O. G. Berg. 1991. Interfacial catalysis by phospholipase A2: dissociation constants for calcium, substrate, products, and competitive inhibitors. *Biochemistry.* **30:** 7306–7317.
8. Kim, T. S., C. S. Sundaresh, S. I. Feinstein, C. Dodia, W. R. Skach, M. K. Jain, T. Nagase, N. Seki, K. Ishikawa, N. Nomura, et al. 1997. Identification of a human cDNA clone for lysosomal type Ca2+-independent phospholipase A2 and properties of the expressed protein. *J. Biol. Chem.* **272:** 2542–2550.
9. Fisher, A. B., C. Dodia, Y. Manevich, J. W. Chen, and S. I. Feinstein. 1999. Phospholipid hydroperoxides are substrates for non-selenium glutathione peroxidase. *J. Biol. Chem.* **274:** 21326–21334.
10. Singh, A. K., and H. Shichi. 1998. A novel glutathione peroxidase in bovine eye. Sequence analysis, mRNA level, and translation. *J. Biol. Chem.* **273:** 26171–26178.
11. Kang, S. W., I. C. Baines, and S. G. Rhee. 1998. Characterization of a mammalian peroxiredoxin that contains one conserved cysteine. *J. Biol. Chem.* **273:** 6303–6311.
12. Chen, J. W., C. Dodia, S. I. Feinstein, M. K. Jain, and A. B. Fisher. 2000. 1-Cys peroxiredoxin, a bifunctional enzyme with glutathione peroxidase and phospholipase A2 activities. *J. Biol. Chem.* **275:** 28421–28427.
13. Mo, Y., S. I. Feinstein, Y. Manevich, Q. Zhang, L. Lu, Y. S. Ho, and A. B. Fisher. 2003. 1-Cys peroxiredoxin knock-out mice express mRNA but not protein for a highly related intronless gene. *FEBS Lett.* **555:** 192–198.
14. Wang, X., S. A. Phelan, K. Forsman-Semb, E. F. Taylor, C. Petros, A. Brown, C. P. Lerner, and B. Paigen. 2003. Mice with targeted mutation of peroxiredoxin 6 develop normally but are susceptible to oxidative stress. *J. Biol. Chem.* **278:** 25179–25190.
15. Wang, Y., S. I. Feinstein, Y. Manevich, Y-S. Ho, and A. B. Fisher. 2004. Lung injury and mortality with hyperoxia are increased in peroxiredoxin 6 gene-targeted mice. *Free Radic. Biol. Med.* **37:** 1736–1743
16. Bortnick, A. E., E. Favari, J. Q. Tao, O. L. Francone, M. Reilly, Y. Zhang, G. H. Rothblat, and S. R. Bates. 2003. Identification and characterization of rodent ABCA1 in isolated type II pneumocytes. *Am. J. Physiol. Lung Cell. Mol. Physiol.* **285:** L869–L878.
17. Fisher, A. B., and C. Dodia. 2001. Lysosomal-type PLA2 and turnover of alveolar DPPC. *Am. J. Physiol. Lung Cell. Mol. Physiol.* **280:** L748–L754.
18. Bligh, E. G., and W. J. Dyer. 1959. A rapid method of total lipid extraction and purification. *Can. J. Med. Sci.* **37:** 911–917.
19. Mitnick, M., B. DeMarco, and J. M. Gibbons. 1980. Amniotic fluid phosphatidylglycerol and phosphatidylinositol separated by stepwise-development thin-layer chromatography. *Clin. Chem.* **26:** 277–281.
20. Marinetti, G. V. 1962. Hydrolysis of lecithin with sodium methoxide. *Biochemistry.* **1:** 350–353.
21. Mason, R. J., J. Nellenbogen, and J. A. Clements. 1976. Isolation of disaturated phosphatidylcholine with osmium tetroxide. *J. Lipid Res.* **17:** 281–284.
22. Fisher, A. B. 1985. The isolated perfused lung. *In* Handbook of Experimental Pharmacology. H. Witschi and J. Brain, editors. Springer-Verlag, Heidelberg, Germany. 149–179.
23. Fisher, A. B., and C. Dodia. 1997. Role of acidic Ca2+-independent phospholipase A2 in synthesis of lung dipalmitoyl phosphatidylcholine. *Am. J. Physiol.* **272:** L238–L243.
24. Fisher, A. B., A. Chander, and C. Dodia. 1990. Modulation of lung surfactant clearance. *Prog. Respir. Res.* **25:** 149–157.
25. Kim, T. S., C. Dodia, X. Chen, B. B. Hennigan, M. Jain, S. I. Feinstein, and A. B. Fisher. 1998. Cloning and expression of rat lung acidic Ca(2+)-independent PLA2 and its organ distribution. *Am. J. Physiol.* **274:** L750–L761.
26. Fisher, A. B., C. Dodia, and A. Chander. 1987. Degradation and reutilization of alveolar phosphatidylcholine by rat lungs. *J. Appl. Physiol.* **62:** 2295–2299.
27. Chander, A., J. Reicherter, and A. B. Fisher. 1987. Degradation of dipalmitoyl phosphatidylcholine by isolated rat granular pneumocytes and reutilization for surfactant synthesis. *J. Clin. Invest.* **79:** 1133–1138.
28. Abe, A., M. Hiraoka, S. Wild, S. E. Wilcoxen, R. Paine 3rd, and J. A. Shayman. 2004. Lysosomal phospholipase A2 is selectively expressed in alveolar macrophages. *J. Biol. Chem.* **279:** 42605–42611.
29. Akiba, S., C. Dodia, X. Chen, and A. B. Fisher. 1998. Characterization of acidic Ca(2+)-independent phospholipase A2 of bovine lung. *Comp. Biochem. Physiol. B Biochem. Mol. Biol.* **120:** 393–404.
30. Rider, E. D., K. E. Pinkerton, and A. H. Jobe. 1991. Characterization of rabbit lung lysosomes and their role in surfactant dipalmitoylphosphatidylcholine catabolism. *J. Biol. Chem.* **266:** 22522–22528.
31. Tsao, F. H., and R. D. Zachman. 1977. Phosphatidylcholine-lysophosphatidylcholine cycle pathway enzymes in rabbit lung. II. Marked differences in the effect of gestational age on activity compared to the CDP-choline pathway. *Pediatr. Res.* **11:** 858–861.
32. Post, M., E. A. Schuurmans, J. J. Batenburg, and L. M. Van Golde. 1983. Mechanisms involved in the synthesis of disaturated phosphatidylcholine by alveolar type II cells isolated from adult rat lung. *Biochim. Biophys. Acta.* **750:** 68–77.
33. Baranska, J., and L. M. van Golde. 1977. Role of lamellar bodies in the biosynthesis of phosphatidylcholine in mouse lung. *Biochim. Biophys. Acta.* **488:** 285–293.
34. Chander, A., A. B. Fisher, and J. F. Strauss 3rd. 1982. Role of an acidic compartment in synthesis of disaturated phosphatidylcholine by rat granular pneumocytes. *Biochem. J.* **208:** 651–658.
35. Chakraborti, S. 2003. Phospholipase A(2) isoforms: a perspective. *Cell. Signal.* **15:** 637–665.
36. Winstead, M. V., J. Balsinde, and E. A. Dennis. 2000. Calcium-independent phospholipase A(2): structure and function. *Biochim. Biophys. Acta.* **1488:** 28–39.
37. Dennis, E. A. 1994. Diversity of group types, regulation, and function of phospholipase A2. *J. Biol. Chem.* **269:** 13057–13060.
38. Ackermann, E. J., and E. A. Dennis. 1995. Mammalian calcium-independent phospholipase A2. *Biochim. Biophys. Acta.* **1259:** 125–136.
39. Kudo, I., and M. Murakami. 2002. Phospholipase A2 enzymes. *Prostaglandins Other Lipid Mediat.* **68–69:** 3–58.
40. Balsinde, J., M. A. Balboa, and E. A. Dennis. 1997. Antisense inhibition of group VI Ca2+-independent phospholipase A2 blocks phospholipid fatty acid remodeling in murine P388D1 macrophages. *J. Biol. Chem.* **272:** 29317–29321.
41. Hite, R. D., M. C. Seeds, A. M. Safta, R. B. Jacinto, J. I. Gyves, D. A. Bass, and B. M. Waite. 2005. Lysophospholipid generation and phosphatidylglycerol depletion in phospholipase A2-mediated surfactant dysfunction. *Am. J. Physiol. Lung Cell. Mol. Physiol.* **288:** L618–L624.
42. Uozumi, N., and T. Shimizu. 2002. Roles for cytosolic phospholipase A2alpha as revealed by gene-targeted mice. *Prostaglandins Other Lipid Mediat.* **68–69:** 59–69.
43. Alcorn, J. F., and J. R. Wright. 2004. Degradation of pulmonary surfactant protein D by *Pseudomonas aeruginosa* elastase abrogates innate immune function. *J. Biol. Chem.* **279:** 30871–30879.
44. Heath, M. F., and W. Jacobson. 1976. Phospholipases A1 and A2 in lamellar inclusion bodies of the alveolar epithelium of rabbit lung. *Biochim. Biophys. Acta.* **441:** 443–452.
45. Franson, R. C., and M. Waite. 1973. Lysosomal phospholipase A 1 and A 2 of normal and bacillus Calmette Guerin-induced alveolar macrophages. *J. Cell Biol.* **56:** 621–627.
46. Leavey, P. J., C. Gonzalez-Aller, G. Thurman, M. Kleinberg, L. Rinckel, D. W. Ambruso, S. Freeman, F. A. Kuypers, and D. R. Ambruso. 2002. A 29-kDa protein associated with p67phox expresses both peroxiredoxin and phospholipase A2 activity and enhances superoxide anion production by a cell-free system of NADPH oxidase activity. *J. Biol. Chem.* **277:** 45181–45187.
47. Rhee, S. G., S. W. Kang, T. S. Chang, W. Jeong, and K. Kim. 2001. Peroxiredoxin, a novel family of peroxidases. *IUBMB Life.* **52:** 35–41.
48. Chander, A., R. G. Johnson, J. Reicherter, and A. B. Fisher. 1986. Lung lamellar bodies maintain an acidic internal pH. *J. Biol. Chem.* **261:** 6126–6131.
49. Hiraoka, M., A. Abe, and J. A. Shayman. 2002. Cloning and characterization of a lysosomal phospholipase A2, 1-O-acylceramide synthase. *J. Biol. Chem.* **277:** 10090–10099.
50. Desai, R., T. D. Tetley, C. G. Curtis, G. M. Powell, and R. J. Richards. 1978. Studies on the fate of pulmonary surfactant in the lung. *Biochem. J.* **176:** 455–462.
51. Jacobs, H., A. Jobe, M. Ikegami, and D. Conaway. 1983. The significance of reutilization of surfactant phosphatidylcholine. *J. Biol. Chem.* **258:** 4159–4165.